SLAC – PUB – 4115
March 1987
E/I

TETRAKIS-(DIMETHYLAMINO)-ETHYLENE: ANALYSIS AND COMPATIBILITY WITH COMMON LABORATORY MATERIALS*

ROBERT T. REWICK, MARY L. SCHUMACHER

SRI International, 333 Ravenswood Ave., Menlo Park, CA 94025

STEPHEN L. SHAPIRO, THOMAS B. WEBER

Stanford Linear Accelerator Center, P.O. Box 4349,
Stanford University, Stanford, CA 94305

MATTEO CAVALLI-SFORZA

Santa Cruz Institute for Particle Physics,
University of California, Santa Cruz, CA 94064

Submitted to *Analytical Chemistry*

* Work supported by the Department of Energy, contract DE – AC03 – 76SF00515 and by the National Science Foundation, Grant PHY85 – 12145.

ABSTRACT

Analytical procedures were developed using GC and GC/MS techniques to determine the purity of commercially available and purified liquid and gaseous tetrakis-(dimethylamino)-ethylene (TMAE). More than 20 components were detected; most were identified from their mass spectral fragmentation patterns. The 6 major TMAE impurities were dimethylamine, tetramethylhydrazine, bis-(dimethylamino)-methane, dimethylformamide, tetramethylurea, and tetramethyloxamide. The major impurities accounted for greater than 99 area % of all impurity components detected.

Electron capture analysis of the major TMAE impurities suggested that tetramethyloxamide and tetramethylurea have relative high electron capture cross sections compared with oxygen.

Liquid TMAE was observed to be generally compatible (less than 1% decomposition) with 27 commonly used metal, polymer, and ceramic laboratory materials. In some cases, however, low concentrations of products were generated that had a high affinity for electron capture. Materials that formed statistically significant amounts of these products were identified.

A technique was developed using GC to measure the major TMAE impurities in a gas flow stream containing TMAE vapor.

1. INTRODUCTION

Tetrakis-(dimethylamino)-ethylene (TMAE), first reported by Pruett et al. (1), is well-known for its strong electron donor properties (2,3), and its ability to chemiluminesce on reaction with oxygen (1,4,5). Kinetic studies have shown that the thermal decomposition (6) and light–producing reactions (7,8) of TMAE are complex; chemiluminescence requires catalysis by protonic materials (9). Indeed, pure TMAE in the absence of a few parts per million of protonic activators such as water and alcohols will not react to any appreciable degree with oxygen (9). In addition, the major oxidation products, tetramethylurea (TMU) and tetramethyloxamide (TMO), act as quenchers for the light emission (4,9).

The following physical properties of TMAE have been reported: melting point, $-4°C$ (10); boiling point, 177°C (11); vapor pressure at 25°C, 0.50 torr (11); refractive index at 20°C, 1.4817 (12); liquid conductivity, 1.4×10^{-16} ohm^{-1} cm^{-1} (12); mass spectrum, major peaks at m/e of 200, 185, and 85 (13); NMR, a singlet at 2.59 ppm relative to tetramethylsilane (10); and chemiluminescence maximum, 486 nm in alkane solvents (14).

The most unusual property of TMAE, however, concerns the electron-rich environment of the TMAE molecule. Excess electrons in TMAE have a mobility of 2.2 cm^2/V-s at 20° C, which is 100 times higher than the mobility of electrons in other amines (14). Moreover, TMAE is readily ionized, a property that makes it useful as a liquid or gaseous photocathode (15,16). TMAE and a series of other related tetraaminoethylenes have low gas-phase first ionization potentials (I_p) close to that reported for the lithium atom, 5.4 eV (17). For example, I_p

reported for TMAE is 5.36 ± 0.02 eV (18).

Because tetraaminoethylenes have low ionization potentials, high quantum efficiencies for absorption of ultraviolet light and ejection of a photoelectron, and adequate vapor pressures, there is much interest in the use of these materials to detect Čerenkov radiation (11, 19). Studies of the electronic properties of TMAE, such as its photoionization cross section (11, 20), combined with its relatively high vapor pressure (11) suggest that TMAE is the ideal member of the tetraaminoethylene family for use in a Čerenkov radiation detector. For this reason, particle physicists in the United States and Europe are actively pursuing the use of TMAE in such detectors.

Because TMAE is readily ionized to radical cations in the presence of trace amounts of oxygen and protonic activators, TMAE is difficult to maintain in the pure state. Indeed, TMAE has been observed to interact with components of a prototype Čerenkov detector system to generate unidentified impurities that strongly absorb the photoelectrons as they drift in the carrier gas (21). For high detector efficiency, TMAE photoejection electrons must have a relatively long lifetime (about 100 μs) in a Čerenkov drift detector. Materials with high electron capture cross sections will severely reduce electron drift lifetimes; for instance, an oxygen concentration of more than 10 ppm in the drift gas produces unacceptably low lifetimes. Because the relative electron affinity of TMAE reaction/decomposition products is not known, it is possible that the presence of these materials contributes to the low electron drift lifetimes occasionally observed in Čerenkov drift detectors.

Aside from numerous reports on reactions of TMAE with oxygen (5, 9, 22, 23),

water (13), methane (13), and π–acceptors, such as pyrene, anthracene, and nitrobenzenes (2), little information is available on interactions of TMAE with laboratory materials frequently used to construct detectors, gas systems, and transfer lines, such as metals, O–rings, and gaskets. In an unpublished report (24), researchers at Rutherford Appleton Laboratory describe the compatibility of liquid TMAE with elastomeric materials for O–ring seals, but do not discuss reaction products. Analytical procedures to identify TMAE reaction products with these materials are not well documented in the literature.

Carpenter and Bens (25) identified some of the oxidation products of TMAE using gas chromatography/mass spectrometry (GC/MS). From a total of at least 35 components detected by GC, only 7 oxidation products were positively identified by MS. However, the analytical techniques used in this work such as details on detectors, sample size, and mass sweep range/rate, are not well described.

Urry and Sheeto (26), using nuclear magnetic resonance (NMR) and mass spectrometry, studied the relative amounts of products formed in the autoxidation of TMAE in various solvents. The results, which were surprisingly independent of both the solvent and the temperature, were as follows: 65% tetramethylurea (TMU), 18% tetramethyloxamide (TMO), 12% tetramethylhydrazine (TMH), and 2% bis-(dimethylamino)-methane (BMAM).

Waring and Berard (6) described a GC system for the analysis of TMAE thermal decomposition products. The results from the analysis, using at least three GC columns, a gas sampling valve, and a vacuum system, suggest the major (98%) products to be methane and dimethylamine (DMA). The thermal decomposition reaction of TMAE is significantly less complex than the oxidation

reaction, which can occur at room temperature to form a wide variety of products such as DMA, TMH, and TMU.

The objective of our study was to develop improved analytical methods to determine TMAE purity and identify products from the interaction of TMAE with typical laboratory materials used to build particle detectors or flow systems. In this work we optimized the GC method for the analysis of TMAE, confirmed the identity of the major impurities by GC/MS, determined by electron capture analysis several impurities that may have sufficient electron affinity (relative to oxygen) to interfere with the detection of photoelectrons produced in a Čerenkov detector, and evaluated the reactivity of liquid TMAE with commonly used metal, plastic, polymeric, and ceramic materials.

2. EXPERIMENTAL SECTION

2.1 TMAE PURIFICATION

TMAE from several suppliers was used in the present work. Samples were purchased from RSA Corp., Ardsley, New York, and from Aldrich Chemical Co., Milwaukee, Wisconsin. Other samples were obtained from Brookhaven National Laboratory, Upton, New York, after purification by a treatment described by Holroyd et al. (12): water washing to remove DMA, TMO, and other water-soluble impurities; drying over 5-Å molecular sieves; passing through a column of silica gel, previously activated at 400°C, under an atmosphere of nitrogen; distilling several times under vacuum from trap (+50°C) to trap (−78°C); and finally storing over NaK alloy for several days. Samples of TMAE from each

successive purification step, except for that stored over NaK, were analyzed at SRI.

TMAE samples, stored in a Vacuum Atmospheres Corp. dry box, Model No. He-43-6, capable of maintaining an inert nitrogen atmosphere with < 1 ppm oxygen and water, were transferred to septum bottles and capped with Mininert valves (Supelco Inc. and Alltech Assoc.) for removing liquid and vapor syringe samples.

2.2 Gas Chromatography

Table I lists the conditions used with a Hewlett-Packard Model HP-5830 for the analysis of TMAE. Four columns were evaluated to achieve maximum identification and separation of TMAE impurities and minimize the possibility that TMAE might interact with the column packing material. The columns were recommended by several suppliers (Supelco Inc., and Alltech Assoc.) and the literature (25) as being suitable for the analysis of amines.

Samples of neat TMAE liquid and vapor from the capped septum bottles were injected by microliter syringe directly on the glass GC columns to avoid TMAE decomposition on the warm metallic injector. To minimize oxidation of TMAE by air in the syringe, several aliquots were withdrawn and discarded; the syringe was then filled to more than the desired injection quantity. Immediately before the sample was injected, the excess TMAE was discharged and the needle wiped with a clean tissue.

Table I. GC Conditions for TMAE Analysis

Instrument:		HP-5830A
Detector:		FID
Column:		Glass, 8 feet × 2 mm I.D.
Packing:	(A)	28% Pennwalt 223 + 4% KOH on 80/100 mesh Gas Chrom R
	(B)	Carbopack B/4% CW 20 M/0.8% KOH
	(C)	10% Apiezon L/2% KOH on 80/100 Mesh Chromosorb W AW
	(D)	20% SE-52 on 100/120 mesh Chromosorb WAW DMCS
Carrier:		Helium, 45 cm^3 min^{-1} (at 50°C)
Temperatures:		
	Injector	100°C
	Detector	225°C
	Column	50°C/3 min $\xrightarrow{10°C/\text{min}}$ 210°C/9 min
Sample Size:		
	Liquid	1 μL
	Vapor	50 μL

2.3 Electron Affinity

An electron capture detector (ECD) was used to measure the relative electron affinity of TMAE impurities. Table II lists the GC conditions used with a Hewlett-Packard Model HP-5890A (ECD equipped) to analyze these materials. The ECD provides a thermal electron source from the ionization of the nitrogen carrier gas; the electrons are collected with a pulsed electric field. The ECD signal is correlated to the decrease in electron current caused by the electron-capturing compounds. Care must be taken to operate in a region where the signal is linearly related to the compound concentration. When this is the case, the ECD response per unit concentration is proportional to the electron capture cross section. Materials producing strong ECD signals, such as oxygen and Freons, (27) will absorb TMAE photoejection electrons and reduce the efficiency of a Čerenkov drift detector.

Because absolute values for electron capture cross sections are difficult to measure by the GC technique, the response of the ECD to major TMAE impurities relative to oxygen was obtained. For these measurements, we used dilute solutions (7-75 ppm) of TMH, BMAM, DMF, TMU, and TMO in high purity hexane (Baker Resi-Analyzed). DMA was not tested because it is difficult to handle and not expected to have a measurable ECD response. Samples of oxygen (6-25 ppm in helium) were injected into the GC from a 1-cm^3 gas sampling loop. The response of the ECD to several concentrations of oxygen and TMAE impurities was necessary to ensure that comparative measurements were taken in the linear range of the detector, *e.g.*, before saturation.

Table II. GC Conditions for ECD Analysis

Instrument:	HP-5890A		
Detector:	ECD		
Column:	DB-5 (1.5 μm) fused silica (15 m $\times$ 530 μm I.D.)		
Carrier:	N_2 (cm^3/min)		
		Column	Make-up
	TMU	5	65
	TMO	60	0
	BMAM, DMF, TMH	9	43
Temperature:			
Injector	100° C		
Detector	225° C		
Column:			
	100°C/5 min $\xrightarrow{75°C/\text{min}}$ 150°C/1 min (TMU, TMO)		
	50°C isothermal (BMAM, DMF, TMH)		
Sample Size:			
	1 μL liquid (TMU, TMO)		
	5 μL vapor (BMAM)		
	10 μL vapor (DMF, TMH)		

2.4 Gas Chromatography/Mass Spectrometry

GC/MS measurements were made using a Ribermag Model R 10-10 (Nermag, France) GC/MS, a 30-meter DB-5-coated capillary column programmed from 50° to 300°C at 10°C min^{-1} and a mass spectral sweep rate of 50 to 300 amu s^{-1}. The instrument, operated in a solvent flush mode, discriminated against volatile low molecular weight (m/e < 50) TMAE components such as DMA because this fraction was lost when a liquid sample was flushed with helium.

2.5 Materials Compatibility

TMAE compatibility tests were conducted by exposing various metal, plastic, and ceramic components in 9-cm^3 septum vials to 1 cm^3 liquid TMAE from RSA Corp. All samples were completely covered by the liquid. Table III describes the solid materials of approximate 200-300 mm^2 surface area and in the case of metals and ceramics, cleaned with water, acetone, and air dried at 125°C. Vapor and liquid TMAE aliquots were withdrawn from the septum vials for GC analysis after at least 24 hours exposure at 23-25°C. If the GC analyses differed significantly from a blank sample, TMAE was considered to interact with the solid substrate.

2.6 Monitoring Impurities in a Gas Stream

Because the ultimate objective of this research was to develop a GC analytical method to monitor the impurities in a TMAE flow stream, we constructed and evaluated a simple prototype flow apparatus to determine the detection level of TMAE impurities. A TMAE vapor stream was established in a stainless steel

Table III. Description of Samples for TMAE Compatibility Testing

I. Metals	Description
1. Stainless Steel (316)	1/4″ O.D. Tubing, Electropolished
2. Copper	1/4″ O.D. Tubing
3. Monel	1/4″ O.D. Tubing
4. Cu-Be	0.002″ Wire
5. Cajon VCR Gasket	Flat O–Ring, No. SS-4-VCR-2-GR
6. Aluminum	1/4″ O.D. Tubing
7. Tin/Lead Solder	0.030″ Wire
II. Plastics	
8. Mylar	0.004″ Sheet
9. Nylon	1/4″ Threaded Rod
10. Polyethylene	1/4″ O.D. Tubing
11. Tygon	0.316″ O.D. Tubing
12. Kapton	0.125″ Sheet
III. Fluorinated Polymers	
13. Teflon	0.062″ Sheet
14. Kalrez	O–Ring
15. Viton	O–Ring
16. Kel-F	0.084″ Sheet
IV. Elastomers	
17. Silicone Rubber	0.116″ Sheet
18. Buna-N Rubber	O–Ring
V. Epoxys	
19. G-10	0.068″ Sheet
20. Shell Epon-820	Disk
21. Polyimide PC Board	0.125″ Sheet
22. Scotch Weld DP-190	Disk
VI. Nupro Valve SS-4H-TW	
23. Stem (SS 316)	0.160″ Rod
24. Bellows (SS 321)	0.316″ O.D. Bellows Tubing
VII. Ceramic and Glass	
25. Macor	1/2″ Plate
26. Quartz	1/4″ O.D. Tubing
27. Micalex	0.170″ Plate

system by flowing high purity helium through a TMAE bubbler at 19°C, thus creating a vapor composition of 420 ppm TMAE. A fraction of this vapor was drawn though a 1 cm^3 gas sample loop attached to a Hewlett Packard 5890 GC that operated under the conditions described in Table IV. The gas sample was drawn through the GC by means of a variable displacement pump, chosen to be impervious to the effects of gaseous TMAE, and protected from ambient air by input and output bubblers.

3. RESULTS AND DISCUSSION

3.1 GC ANALYSIS

Figure 1 shows GC spectra of TMAE from RSA Corp. analyzed on four column packing materials. The major impurities were identified by comparing their retention times to those of known materials analyzed under identical conditions. Symbols used to represent the major peaks are given in Table V. As shown in Figure 1, Column A vapor pressure was excessive above about 155°C; only DMA and incompletely separated TMH and BMAM were identified at lower temperatures. For Column B, TMAE or its impurities interacted with the packing material above about 100°C. This was verified at higher detector attenuation levels where unidentified peaks were visible. In addition, Column B had to be heated for about 1 hour at 210°C following each TMAE injection before the baseline returned to its normal value. Column C provided good separation and stability for TMAE. TMH, however, could not be positively identified on Column C because it appeared to co-elute with BMAM as a slight shoulder not visible

Table IV. GC Conditions for FID Analysis of TMAE in Gas Stream

Instrument:	HP-5890A
Detector:	FID
Column:	DB-5 (1.5 μm) Fused Silica (15 m $\times$ 530 μm I.D.)
Carrier:	He
	Column: 8.5 cm^3/min; Make-up: 16.5 cm^3/min
Temperature:	
Injector	70°C
Detector	225°C
Column:	38°C/3 min $\xrightarrow{10°C/\text{min}}$ 210°C
Sample Size:	1 cm^3 Valco sample loop at 30°C

on the artist's version of the spectrum. Column D provided the best separation of major TMAE components; the TMAE peak, however, tailed more than on Column C, which could mask hidden peaks or affect integration accuracy.

The similar GC results observed on Columns C and D suggest that both columns are useful for the analysis of TMAE. Area percent calculations contain the uncertainty associated with the absence of response factors for each component. Such calibrations are usually difficult for complex mixtures such as TMAE. Although the number of TMAE impurities detected by Column D is somewhat greater than Column C, the six major identified components represent over 99.5 area % of the sample. None of the remaining unidentified impurities was present to an extent greater than 0.03 area %.

Figure 2 shows the vapor-phase GC spectrum of TMAE taken from the headspace above a liquid sample. Most peaks were identified by GC (Peaks 1-7) or GC/MS (Peaks A-F). The vapor spectrum contained fewer detectable components than the liquid spectrum [Figure 1(d)] and was enriched in volatile components such as DMA, TMH, BMAM, DMF, and TMU, with a corresponding reduction in the concentration of TMAE. Table VI describes various physical properties of TMAE and its major impurities. As shown, the measured vapor pressure for TMO is nearly the same as that reported for TMAE. A comparison of the liquid and vapor phase compositions of TMAE from two suppliers given in Table VII shows that the vapor phase above liquid TMAE is enriched in TMO. It is possible that higher vapor phase concentrations of TMO may result from reaction of TMAE vapor and air in the syringe before the sample is injected into the GC.

Table V. Symbol Identification

Symbol	Name	Formula	MW
DMA	Dimethylamine	$(CH_3)_2NH$	45
TMH	Tetramethylhydrazine	$(CH_3)_2 - N - N(CH_3)_2$	88
BMAM	Bis(dimethylamino)methane	$[(CH_3)_2N]_2 - CH_2$	102
DMF	Dimethylformamide	$H(C=O) - N(CH_3)_2$	73
TMU	Tetramethylurea	$[(CH_3)_2N]_2 - C=O$	116
TMAE	Tetrakis(dimethylamino)ethylene	$C_2[(CH_3)_2N]_4$	200
TMO	Tetramethyloxamide	$[(CH_3)_2N]_2 - (C=O)_2$	144

Table VI. Physical Properties of TMAE and Major Impurities

Compound	Formula	MW	MP (°C)	BP (°C)	VP (torr)$^{°C}$	Density (g/cm^3)$^{°C}$	Refractive Index (n_D)$^{°C}$
DMA	C_2H_7N	45	[a] -92	[a] 6.9	[b] 1520^{25}	[a] 0.6804^{0}	[a] 1.350^{17}
TMH	$C_4H_{12}N_2$	88		[c] 73-74	[d] 87.5^{22}	[e] 0.777	[e] 1.414
BMAM	$C_5H_{14}N_2$	102		[a] 85	[d] 74.0^{23}	[a] 0.749^{25}	[a] 1.4005^{20}
DMF	C_3H_7NO	73	[a] -61	[a] 153	[d] 3.5^{23}	[a] 0.9445^{25}	[a] 1.4269^{25}
TMU	$C_5H_{12}N_2O$	116	[a] -1	[a] 177.5	[d] 1.4^{d}	[a] 0.972^{15}	[a] 1.4506^{20}
TMAE	$C_{10}H_{24}N_4$	200	[f] -4	[g] 177	[g] 0.50^{25}	[f] 0.861^{25}	[b] 1.4817^{20}
TMO	$C_6H_{12}N_2O_2$	144	[h] 78-79		[d] 0.39^{23}		

[a] Reference 17.

[b] Reference 12.

[c] Reference 28.

[d] Measured at SRI with an MKS Baratron capacitance manometer.

[e] Reference 29.

[f] Reference 10.

[g] Reference 11, $\log_{10}$ P (torr) = 9.102–2802.43/T.

[h] Measured at SRI with a Fisher-Johns melting point apparatus.

Table VII. Analysis of TMAE from Two Different Suppliers[a]

(area %)

Supplier	RSA Corp.		Aldrich Chem. Co.	
Impurity	Liquid	Vapor	Liquid	Vapor
DMA	0.15	11.35	0.10	20.68
TMH	0.11	1.24	0.35	2.23
BMAM	0.44	2.31	1.39	5.44
DMF	0.08	0.14	trace	0.11
TMU	0.31	2.78	1.04	3.14
TMAE	98.56	80.35	96.51	65.69
TMO	0.04	0.87	0.01	1.47

[a] Stored over dried 3 Å molecular sieve GC Column D.

Figure 3 shows GC spectra of TMAE from RSA Corp. after a series of purification treatments. Based on these procedures, the analyzed purity of TMAE increased from 98.87 to 99.96 area %, with substantial reduction in the concentration of the major oxidation products, TMU and TMO. The results are summaried in Table VIII. Qualitatively, TMAE chemiluminescence increased with purity; light generation was visibly enhanced with 99.96 area % TMAE when a sample was sprayed on a piece of white paper in the open-air laboratory, as expected. Oxidation product impurities, such as TMU and TMO, have been reported to inhibit the reaction of TMAE with oxygen (4, 9).

3.2 GC/MS Analysis

The GC/MS spectrum of TMAE (Figure 4) was generally similar to the GC spectrum [Figure 1(d)]. The elution order of major components on the GC/MS capillary column (DB-5 liquid phase) was nearly identical, but with enhanced separation, compared to the GC packed column (SE-52 liquid phase). In Figure 4, a chemical structure or molecular weight is assigned to each peak according to its observed mass spectral cracking pattern (Figure 5). In some cases, no peak assignments were possible because of the absence of library reference data; for other peaks, question marks indicate that the assignment is subject to some uncertainty.

In the GC/MS spectrum for TMAE (Figure 4), the peak for DMA is not shown because the GC/MS operates in a solvent flushing mode (high volatility components are lost) and the mass spectral scan begins above the molecular weight of DMA. The presence of DMA was confirmed, however, when the scan

Table VIII. Effect of Purification Treatment on TMAE Purity[a]

(area %)

	Treatment[b]			
Product	1	2	3	4
DMA	0	0	trace	0
TMH	0.04	0.03	trace	trace
BMAM	0.50	0.03	trace	trace
DMF	0.07	0.01	0.01	trace
TMU	1.28	0.14	trace	trace
TMAE	98.87	99.62	99.90	99.96
TMO	0.03	0.01	0.01	0.01

[a] Liquid sample; GC column D; see Figure 3 for spectra.

[b] 1. As received from RSA Corp.

2. Washed with water, molecular sieve.

3. Washed with water, molecular sieve, silica gel.

4. Washed with water, molecular sieve, silica gel, vacuum distilled.

range was temporarily increased and the flush stream was stopped; DMA is shown in Figure 4 at its approximate elution time.

Several impurity components thought to arise during TMAE preparation or handling were evident in the GC/MS spectrum: pyridine (Peak 5) and silicone oil (Peaks 7 and 9). The tentative assignment made for Peak 8, a methyloxamide derivative, seemed reasonable because of the relative high abundance of a related oxidation product, TMO (Peak 17).

Tetramethylurea, Peak 10, was a major TMAE impurity, but appeared to tail rather badly on the DB-5 capillary column. However, the mass spectrum remained constant for TMU during this tailing period, suggesting that other peaks were not co-eluting.

Following TMAE (Peak 13), Peaks 14, 15, and 16 were assigned structures that were related to that of TMAE. That is, the three components probably have the bis(dimethylamino)ethylene linkage, but also a mixed methylamino group on the second carbon. It is likely that these impurities were generated during the TMAE synthesis procedure and are not products from hydrolysis or oxidation.

Following TMO (Peak 17), small unidentified products (Peaks 18-23) were observed. Although the parent ion (M^+) was apparent, the observed fragmentation patterns did not match that of any known materials in our reference library.

In general, the mass spectral work of Carpenter and Bens (25) did not aid the interpretation of our tentative or unknown structural assignments. Agreement between the two experiments was not necessarily expected because of possible differences in the two ionization energy sources, mass scan ranges, and degree of

oxidation of the TMAE samples.

The composition of TMAE vapor is easier to describe than the liquid because fewer peaks are observed. In the vapor phase spectrum (Figure 2), all the major peaks can be positively identified or given tentative structure or molecular weight assignments. The analysis accounts for > 99.9 area % of the sample.

3.3 Electron Affinity Results

As described in Table II, ECD analyses of TMAE impurities and oxygen were made to determine which materials had electron capture cross sections of the same order or larger than that of oxygen and thus are particularly undesirable when photoelectron drift must be maximized. Of the major TMAE impurities, BMAM, DMF, and TMH did not produce a clear ECD signal; TMO and TMU, however, produced normalized responses in area counts per molecule of several times that of oxygen and of the same order as oxygen respectively. The results, however, are only qualitative because of analytical difficulties in repeating the measurements. Work is in progress to obtain quantitative information; the results will be the subject of a future publication.

3.4 Materials Compatibility

TMAE compatibility results were based on differences observed in GC spectra of TMAE in the presence and absence of a given laboratory material. Analytical precision for the six major TMAE impurities were obtained from 5 to 7 replicate analyses of the TMAE blank. For liquid-phase measurements, standard deviations ranged from a few tenths to several percent of the mean for most TMAE

components. For example, five replicate blank analyses of liquid TMAE from RSA Corp. gave a value of 98.56 ± 0.17 area % TMAE (Table VII).

Vapor-phase measurements were not as precise as liquid-phase measurements. Headspace syringe analyses are usually difficult because of problems encountered with aerosol formation, sample fractionation, condensation, and air contamination. For example, seven replicate blank analyses of TMAE vapor gave a value of 80.35 ± 11.08 area % TMAE (Table VII).

Because the relative precision for the concentration of liquid- and vapor-phase components in the TMAE blank differed widely, we chose the following criteria to evaluate the TMAE compatibility test results: vapor phase results were considered significant if the concentration of an impurity in the vapor phase exceeded the mean value of the same impurity in the blank by more than two standard deviations, whereas the liquid-phase results were considered significant if the mean value exceeded one standard deviation.

For example, TMAE in the presence of G-10, generated 19.33 area % TMU in the vapor phase (Table IX). The blank contained 5.08 ± 2.79 area % TMU; the rating parameter, mean plus two standard deviations, is 10.66. Hence, the concentration of TMU in the vapor phase, generated from contact of TMAE with G-10, exceeded this value, and the stability of TMAE in the presence of this solid is suspect. TMAE test results with high rating factors for vapor and liquid phase analyses are given in Tables IX and X, respectively.

Based on our arbitrary rating system, TMAE may interact with the materials shown in Tables IX and X. Such interactions, however, are small; in no case did

TMAE-purity decrease by more than 1 area % in the presence of any test material.

The formation of TMU was observed with TMAE exposure to most of the solids tested, but was not considered a reliable indicator of TMAE/solid interaction because TMU is the major TMAE oxidation product (25); small amounts of surface oxides, water, or other residues left on the substrate surface could account for the formation of TMU. The formation of TMO was considered a more significant indicator of TMAE/solid interaction because it was generally observed to be high in only a few cases: Nylon and Micalex in the vapor phase (Table IX) and in the liquid phase (Table X) Buna-N rubber, Nupro valve bellows, and Macor. Qualitatively, the appearance of the TMAE/solid mixture changed with silicone rubber (substrate swelled) and nylon (TMAE color change). In all other cases, no visible evidence of TMAE reaction was observed.

Because electron capture results suggest that TMO has a relative high electron capture affinity compared with oxygen, materials that generate TMO should not be used in the construction of a Čerenkov drift detector. Other materials to avoid using in the presence of liquid TMAE are those that exceed both liquid and vapor phase rating limits (Table IX and X), namely, G-10, Kel-F, Kalrez, the Nupro valve stem, and Nylon.

3.5 Flow Stream Analysis

Figure 6 shows the GC spectrum of a TMAE–saturated (420 ppm) He flow stream obtained by bubbling He through liquid TMAE at 19°C and injecting a sample loop aliquot. From peak response factors and pressure/volume characteristics of the loop, we estimate that Peak 6, thought to be $[CH_3)_2N]_2$

$C = CHN(CH_3)_2$, is present at a concentration of $\sim$ 50 ppb. Because peaks with areas of about a factor of 2-3 less than Peak 6 can easily be detected, we suggest that the GC flow analysis is sensitive to TMAE impurities at a concentration level of $\sim$ 15-25 ppb. These results imply that the GC flow method used on a TMAE flow stream will easily detect the presence of TMAE impurities that might interfere with electron drift measurements.

4. CONCLUSIONS

4.1 GC ANALYSIS

GC conditions were optimized, using an SE-52/Chromosorb column, to analyze liquid and vapor samples of TMAE from two commercial suppliers and samples purified by distillation and treatment with selective absorbents. The purity of these TMAE liquid samples ranged from 96.51 to 99.96 area %. More than 20 components were detected in TMAE by GC analysis; the six major impurities are dimethylamine, tetramethylhydrazine, bis-(dimethylamino)-methane, dimethylformamide, tetramethylurea, and tetramethyloxamide. Vapor-phase analysis showed the presence of about 80 area % TMAE with enrichment in the more volatile components. Vapor pressure measurements, Table VII, made for all major TMAE impurities, suggested that TMO is nearly as volatile as TMAE.

Table IX. Vapor-Phase Results for TMAE Compatibility Tests[a]

(area %)

	Impurity Analysis		
Sample	TMH	TMU	TMO
G-10	6.50	19.33	–
Kel-F	–	11.12	–
Nupro Valve Stem[b]	–	13.78	–
Nylon	6.24	11.85	1.62
Viton	–	15.66	–
Teflon	3.30	14.19	–
Kalrez	3.38	–	–
Epon-820	3.36	–	–
Silicone Rubber	–	11.14	–
Micalex	–	–	1.24
Blank Mean + 2 S.D.	2.94	10.66	1.23

[a] Greater than blank mean + 2 standard deviations (S.D.).

[b] May be due to traces of cutting oil left on the sample.

Table X. Liquid-Phase Results for TMAE Immersion Tests[a]

(area %)

	Impurity Analysis					
Sample	DMA	TMH	BMAM	DMF	TMU	TMO
G-10		0.24			1.07	
Kel-F		0.23			0.90	
Stainless Steel		0.25			1.09	
Kalrez		0.27		0.10	1.14	
Nupro Bellows[b]					1.00	0.18
Nupro Stem[b]	0.16				0.93	
Nylon		0.23			1.09	
Cu-Be		0.17	0.61		0.94	
Mylar						
Macor					0.84	0.18
Polyethylene					0.87	
Buna-n	0.18					0.23
Aluminum			0.60		0.83	
Cajon Gasket			0.60		0.84	
Monel			0.59		0.83	
Quartz			0.58		0.89	
Copper			0.60		0.90	
Blank Mean + 1 S.D.	0.15	0.17	0.57	0.09	0.79	0.18

[a] Greater than blank mean + 1 standard deviation (S.D.).

[b] May be due to traces of cutting oil left on the sample.

4.2 GC/MS Analysis

Additional TMAE components were identified by GC/MS analysis, including materials thought to arise in TMAE handling or synthesis, such as silicone oil and pyridine. Structural or molecular weight assignments, based on the mass spectral fragmentation pattern for each peak, were made for the 23 major impurities identified in TMAE. The combination of the two analytical techniques, GC and GC/MS, described the composition of TMAE to greater than 99.9 area %.

4.3 Electron Affinity

ECD measurements indicate that TMO has the largest relative electron capture cross section compared with oxygen of any of the major TMAE impurities. Except for TMU, which has an electron affinity about the same as oxygen, other major TMAE impurities exhibit low capture cross section values.

Some caution must be used in correlating ECD results to conditions in a Čerenkov drift detector where electrons drift in electric fields typically between 0.1 and 1 kV/cm. The ECD detector generates thermal electrons ($\sim$ 0.04 eV), whereas the average energy of drifting electrons is typically 0.1 to 0.2 eV. Assuming that ratios of electron capture cross sections of TMO and TMU to oxygen do not change significantly in the specified energy range, the conclusion of our work is that the presence of TMO and TMU impurities in TMAE or impurities generated from contact with reactive system components should be minimized because they are efficient electron scavengers relative to oxygen and may interfere with photoelectron detection when appreciable drift lengths are required.

4.4 - MATERIALS COMPATIBILITY

The reactivity of liquid TMAE with 27 commonly used laboratory materials was measured by GC analysis of the liquid and the vapor headspace above the sample. In all cases, less than 1% TMAE decomposition was observed, suggesting that TMAE is generally compatible with a wide range of materials. However, small concentrations of electron absorbing impurities, such as TMO were observed. A statistical evaluation of the test results, based on the relative precision of GC measurements for blank samples, suggested that TMAE may react with some materials to generate low but significant concentrations of key impurities. Nylon, Micalex, Macor, Buna-N rubber, and the bellows of the Nupro valve formed TMO in the presence of liquid TMAE, while other products were generated in significant amounts with liquid TMAE and G-10, Kel-F, Kalrez, Nylon, and the stem of the Nupro valve. Impurities associated with the Nupro valve stem and bellows may be due to traces of cutting oil left on the sample after cleaning.

Materials tested in the Rutherford Appleton Laboratory (RAL) compatibility study (24) generally included polymers used for O–ring seals. The RAL compatibility test was different from the SRI/SLAC method in that parameters evaluated included weight changes, physical size, physical appearance, and hardness testing on samples exposed to liquid TMAE. Although the SRI/SLAC study also noted physical appearance changes (*e.g.*, swelling of test specimens), emphasis was placed on detection of gas- and liquid-phase TMAE reaction products with the materials under investigation. The RAL report did not describe the purity of the TMAE used in the study; TMAE purity before and after materials eval-

uation was of key importance in the SRI/SLAC work. Thus, the values of the RAL results appear to focus on elastomeric seals to protect TMAE from the environment, whereas the SRI/SLAC work expands the study of other materials of construction.

Of key importance in the SRI/SLAC study is information on the analysis of TMAE and the formation of reaction products that might reduce electron drift lifetimes. The general conclusion from the SRI/SLAC study is that, based on the observed percent decomposition of TMAE in the presence of all test specimens, TMAE is compatible with a wider range of test materials than implied from the RAL report. A color change, the adsorption of TMAE, or swelling do not necessarily indicate that a material cannot be successfully used with TMAE. For example, RAL observed a 122 wt% increase and a yellow color change when Teflon was exposed to liquid TMAE. SRI/SLAC report, $< 1\%$ decomposition of TMAE in the presence of Teflon with the formation of insignificant quantities of reaction products. Both the RAL and SRI/SLAC studies, however, provide generally consistent results that expand current knowledge on the compatibility of TMAE with a broad range of materials.

4.5 Flow Steam Analysis

Results from the GC analysis of 1 cm^3–atm aliquots of a TMAE-in-He flow stream suggest that the detection level for typical TMAE impurities, such as TMO and TMU, is about 15-25 ppb. Based on this sensitivity, we predict that the GC method, in the form of a continuous flow stream monitor, can be used with a Čerenkov detector using TMAE as the gaseous photocathode to monitor

the presence of harmful TMAE impurities arising from leaks or reaction with system components.

Acknowledgement

We are indebted to Robert Reif for his excellent technical help.

LITERATURE CITED

(1) Pruett, R. L.; Barr, J. T.; Rapp, K. E.; Bahner, C. T.; Gibson, J. D.; and Lafferty, R. H.; J. Am. Chem. Soc., 1950, 72, 3646.

(2) Hammond, P.R.; Knipe, R. H.; J. Am. Chem. Soc., 1967, 89, 6063.

(3) Wiberg, N.; Buchler, J. W.; Chem. Ber., 1964, 97(2), 618.

(4) Winberg, H. E.; U.S. Patent 3, 264, 221 (1966).

(5) Freeman, T. M.; Seltz, W. R.; Anal. Chem., 1981, 53, 98.

(6) Waring, C. E.; Berard, R. A.; J. Phys. Chem, 1976, 80 1025.

(7) Fletcher, A. N.; Heller, C. A.; J. Catal., 1966, 6 263.

(8) Fletcher, A. N.; Heller, C. A.; J. Phys. Chem., 1967, 71, 1507.

(9) Winberg, H. E.; Downing, J. R.; Coffman, D. D.; J. Am. Chem. Soc., 1965, 87, 2054.

(10) Holroyd, R. A.; Brookhaven National Laboratory, unpublished results.

(11) Anderson, D. F.; IEEE Trans. Nuc. Sci., 1981, NS-28, 842.

(12) Holroyd, R. A.; Ehrenson, S.; Preses, J. M.; J. Phys. Chem., 1985, 89, 424.

(13) Norris, W. P.; Tetrahedron, 1972, 28, 1965.

(14) Nakato, Y.; Ozaki, M.; Tsubomura, H.; J. Phys. Chem., 1972, 76, 2105.

(15) Kuwata, K.; Geske, D. H.; J. Am. Chem. Soc., 1964, 86, 2101.

(16) Anderson, D. F.; Phys. Lett., 1982, 118B, 230.

(17) "Handbook of Chemistry and Physics," 54th Edition, CRC Press: Cleveland, Ohio, 1973-1974.

(18) Nakato, Y.; Chiyoda, T.; Tsubomura, H.; Bull Chem. Soc. Japan, 1974, 47 3001.

(19) Melchart, G.; Charpak, G.; Sauli, F.; IEEE, Trans. Nucl. Sci., 1980, NS-27, 124.

(20) Nakato, Y.; Ozaki, M.; Tsubomura, H.; Bull. Chem. Soc. Japan, 1972, 45, 1299.

(21) Ashford, V., et al.; IEEE, Trans. Nucl. Sci., 1986, NS-33, 113.

(22) Heller, C. A.; Fletcher, A. N.; J. Phys. Chem., 1965, 69, 3313.

(23) Fletcher, A. N.; Heller, C. A.; J. Phys. Chem., 1967, 71, 1507.

(24) Carolan, P.; Evans, D.; unpublished report, Rutherford Appleton Laboratory, RAL Chemical Technology Division, "The Use of TMAE as a Photoionizing Gas Additive and its Effects on Various Materials used for Dynamic Seals," 1983.

(25) Carpenter, W.; Bens, E. M.; Tetrahedron, 1970, 26, 59.

(26) Urry, W. H.; Sheeto, J.; Protochem. Photobiol., 1965, 4, 1067.

(27) Hunter, S. R.; Christophorou, L. G.; J. Chem. Phys. 1984, 80, 6150.

(28) Durig, J. R.; McNamee, R. W.; Knight, L. B.; Harris, W. C.; Inorg. Chem., 1973, 12, 804.

(29) Fluke Chemicals Catalog 14.

FIGURE CAPTIONS

Fig. 1. GC Separation of components of commercial TMAE with four column packings.

Fig. 2. Vapor-phase GC spectrum of TMAE taken from the headspace above a liquid sample. *Assignments made by GC standards and confirmed by GC/MS. †Assignments made from GC/MS results.

Fig. 3. GC spectra of TMAE from RSA Corp. as purchased and after the indicated purification steps.

Fig. 4. GC/MS spectrum of TMAE.

Fig. 5. Mass spectral cracking pattern of each peak appearing in the GC/MS spectrum of Fig. 4.

Fig. 6. GC spectrum of helium bubbled through TMAE at 19°C.

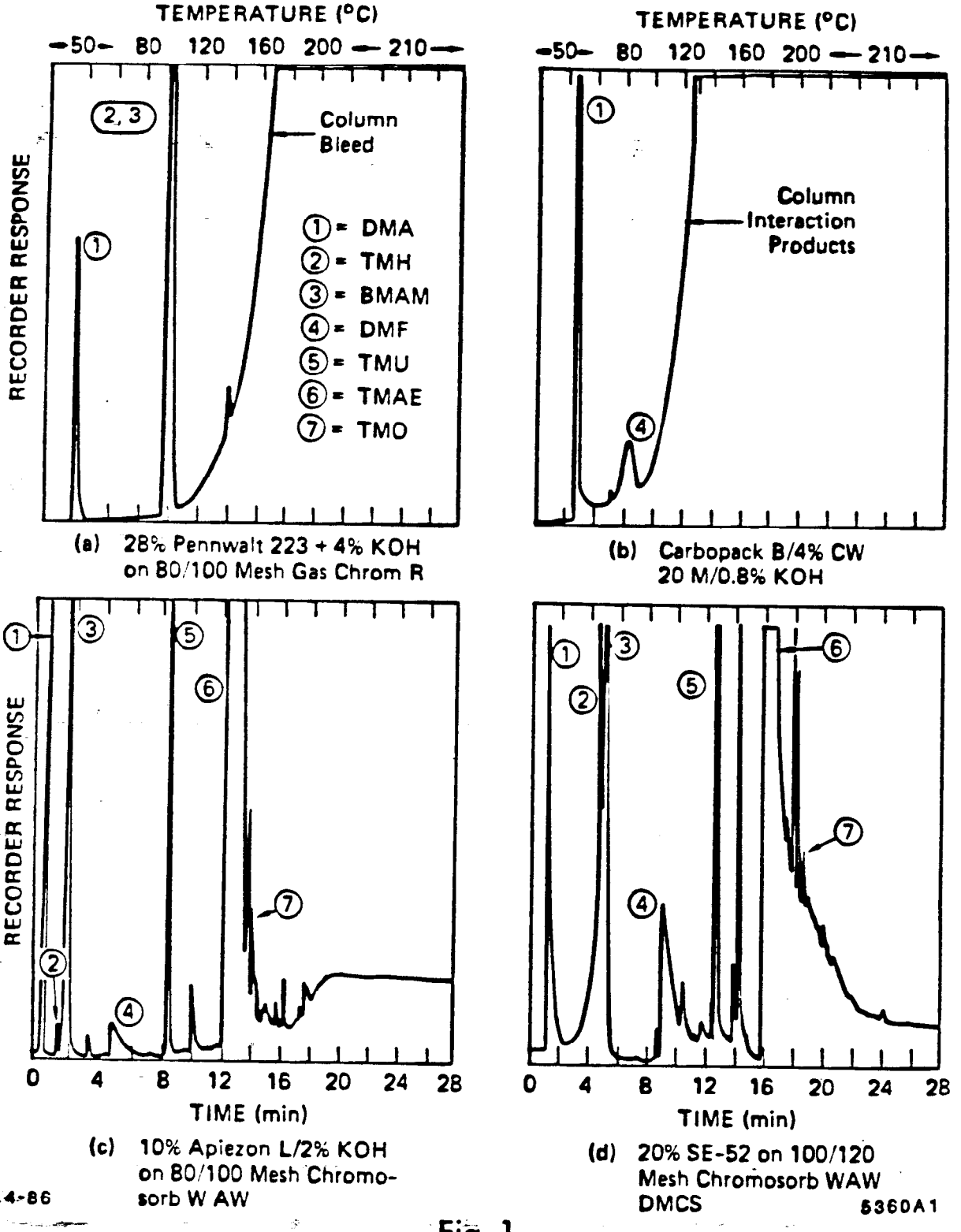
TEMPERATURE (°C)
-50- 80 120 160 200 — 210—
RECORDER RESPONSE
2, 3
Column Bleed
① = DMA
② = TMH
③ = BMAM
④ = DMF
⑤ = TMU
⑥ = TMAE
⑦ = TMO
(a) 28% Pennwalt 223 + 4% KOH on 80/100 Mesh Gas Chrom R
TEMPERATURE (°C)
-50- 80 120 160 200 — 210—
Column Interaction Products
(b) Carbopack B/4% CW 20 M/0.8% KOH
RECORDER RESPONSE
0 4 8 12 16 20 24 28
TIME (min)
(c) 10% Apiezon L/2% KOH on 80/100 Mesh Chromosorb W AW
0 4 8 12 16 20 24 28
TIME (min)
(d) 20% SE-52 on 100/120 Mesh Chromosorb WAW DMCS
4-86
5360A1

Fig. 1

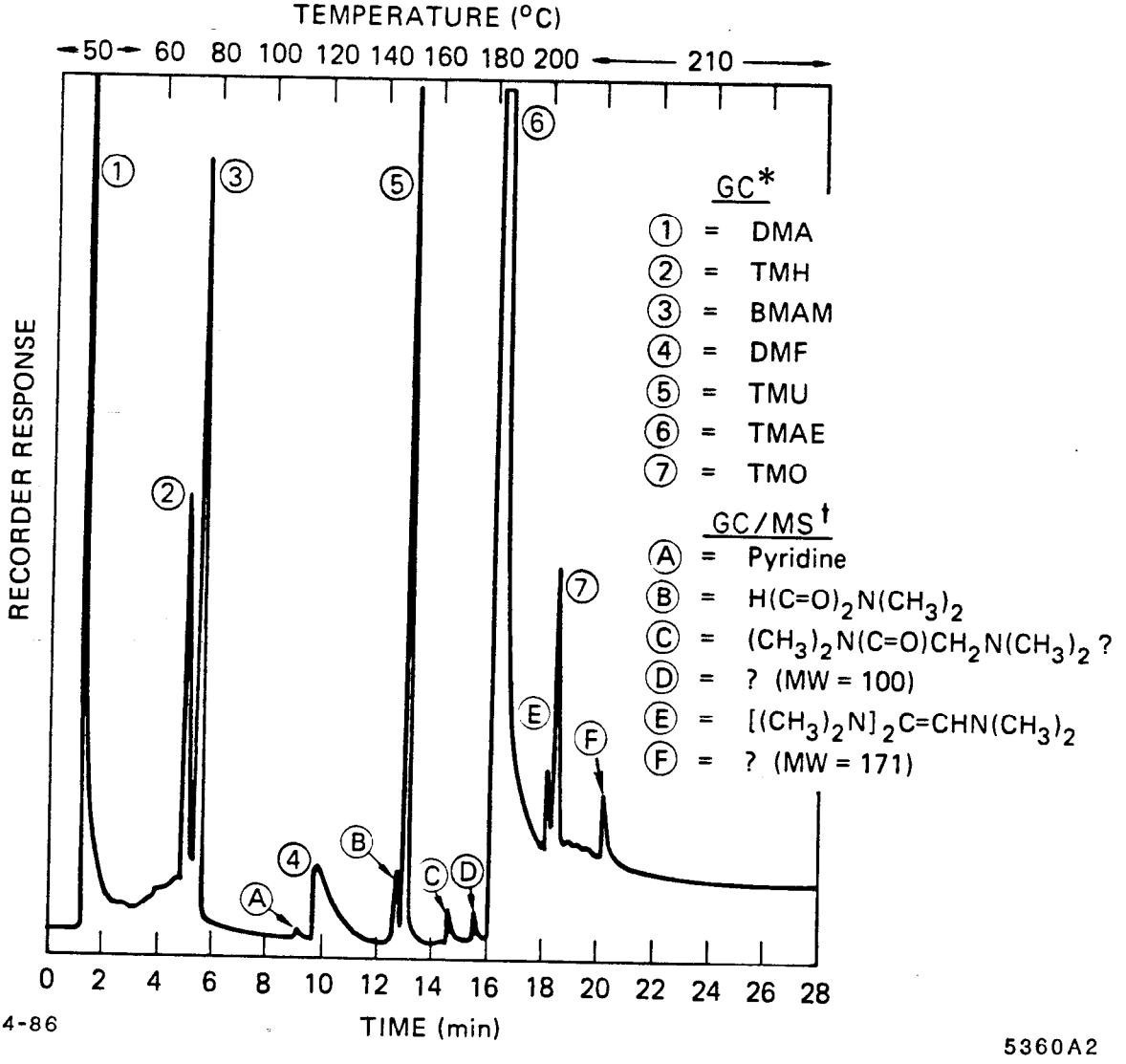
TEMPERATURE (°C)
50 60 80 100 120 140 160 180 200 210
RECORDER RESPONSE
0 2 4 6 8 10 12 14 16 18 20 22 24 26 28
TIME (min)
4-86
5360A2
GC*
① = DMA
② = TMH
③ = BMAM
④ = DMF
⑤ = TMU
⑥ = TMAE
⑦ = TMO
GC/MS†
Ⓐ = Pyridine
Ⓑ = H(C=O)2N(CH3)2
Ⓒ = (CH3)2N(C=O)CH2N(CH3)2 ?
Ⓓ = ? (MW = 100)
Ⓔ = [(CH3)2N]2C=CHN(CH3)2
Ⓕ = ? (MW = 171)

Fig. 2

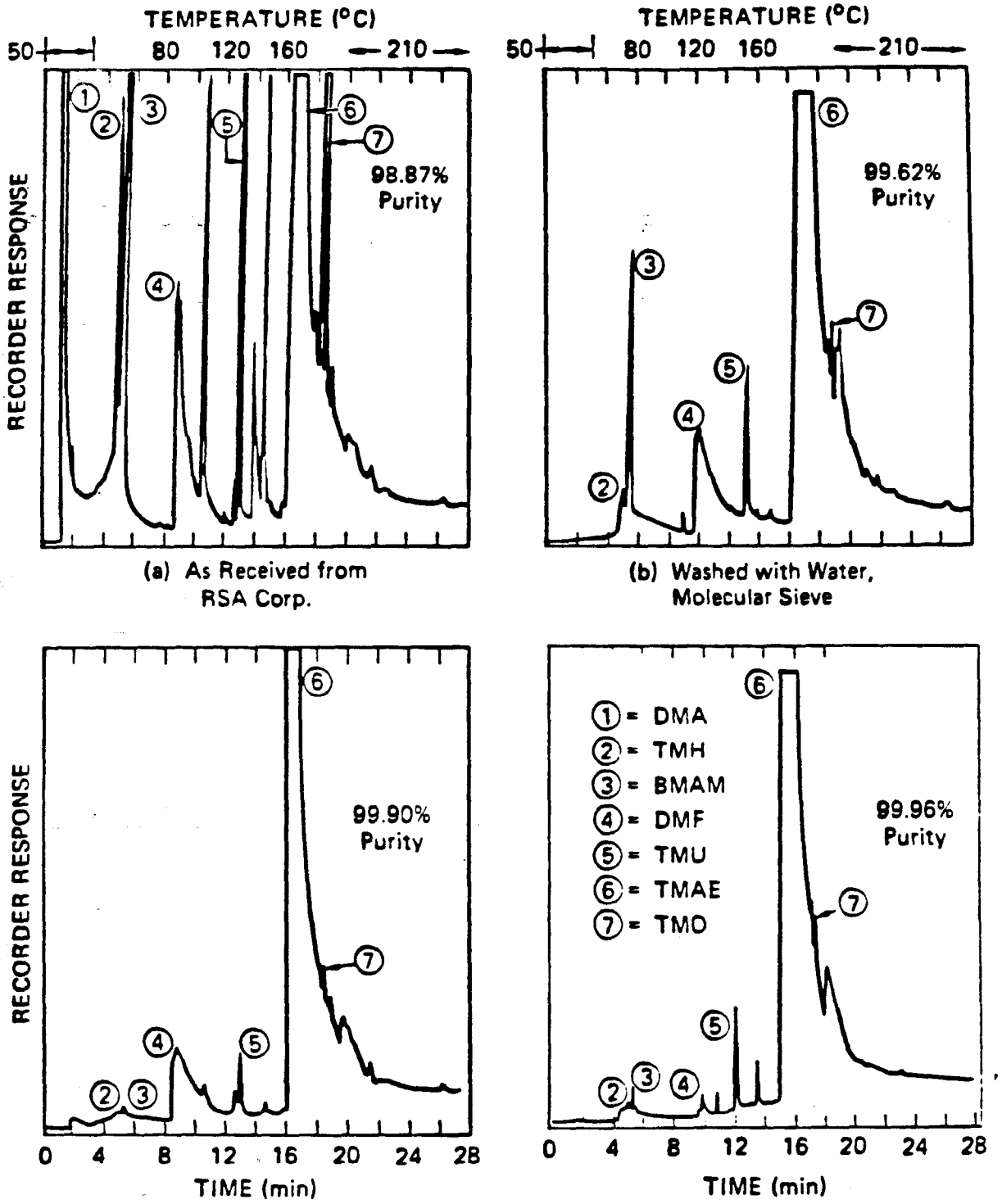

(a) As Received from RSA Corp.

(b) Washed with Water, Molecular Sieve

(c) Washed with Water, Molecular Sieve, Silica Gel

(d) Washed with Water, Molecular Sieve, Silica Gel, Distilled

4-86

5360A6

Fig. 3

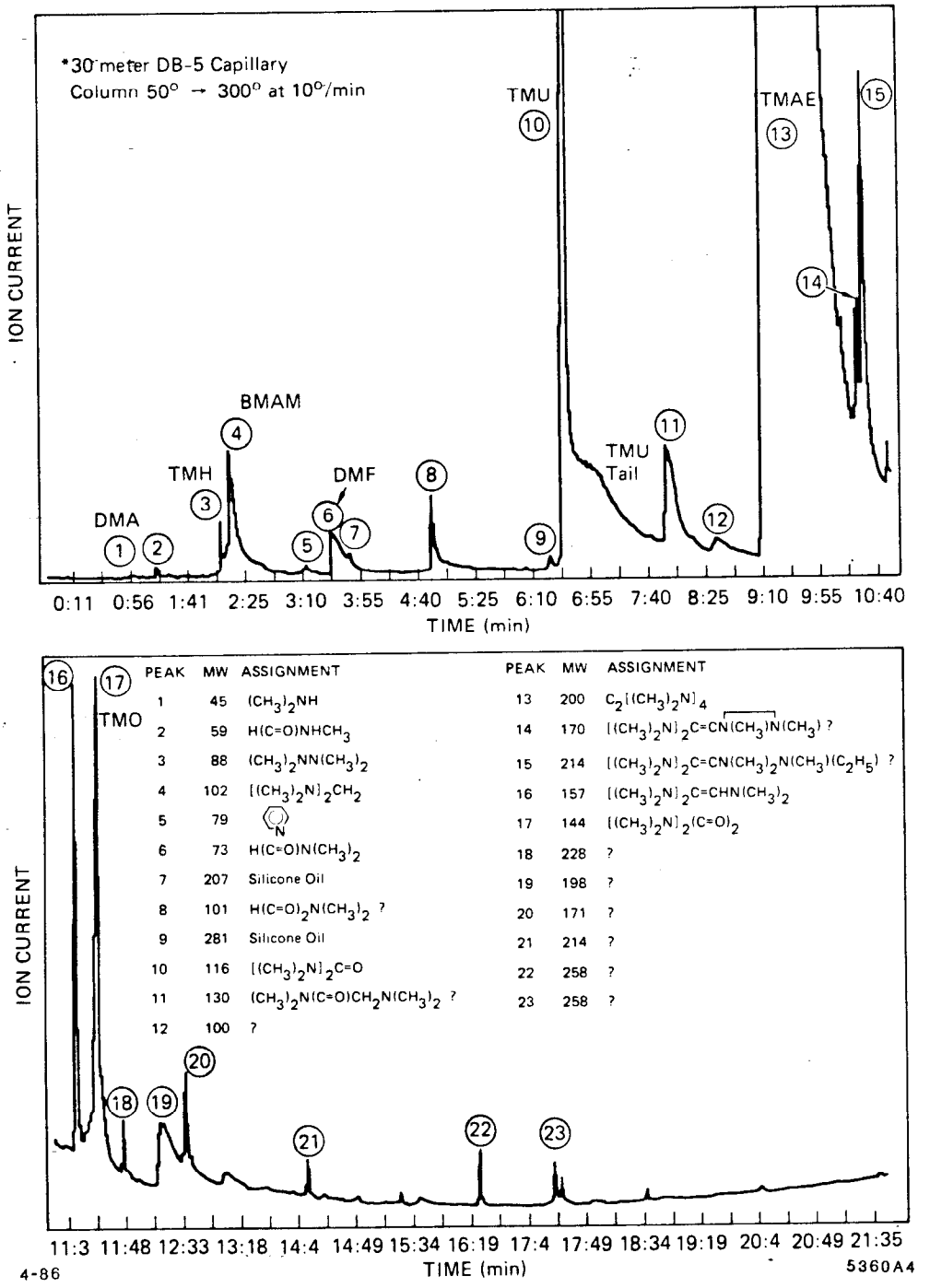

PEAK	MW	ASSIGNMENT
1	45	$(CH_3)_2NH$
2	59	$H(C{=}O)NHCH_3$
3	88	$(CH_3)_2NN(CH_3)_2$
4	102	$[(CH_3)_2N]_2CH_2$
5	79	
6	73	$H(C{=}O)N(CH_3)_2$
7	207	Silicone Oil
8	101	$H(C{=}O)_2N(CH_3)_2$?
9	281	Silicone Oil
10	116	$[(CH_3)_2N]_2C{=}O$
11	130	$(CH_3)_2N(C{=}O)CH_2N(CH_3)_2$?
12	100	?
13	200	$C_2[(CH_3)_2N]_4$
14	170	$[(CH_3)_2N]_2C{=}CN(CH_3)N(CH_3)$?
15	214	$[(CH_3)_2N]_2C{=}CN(CH_3)_2N(CH_3)(C_2H_5)$?
16	157	$[(CH_3)_2N]_2C{=}CHN(CH_3)_2$
17	144	$[(CH_3)_2N]_2(C{=}O)_2$
18	228	?
19	198	?
20	171	?
21	214	?
22	258	?
23	258	?

Fig. 4

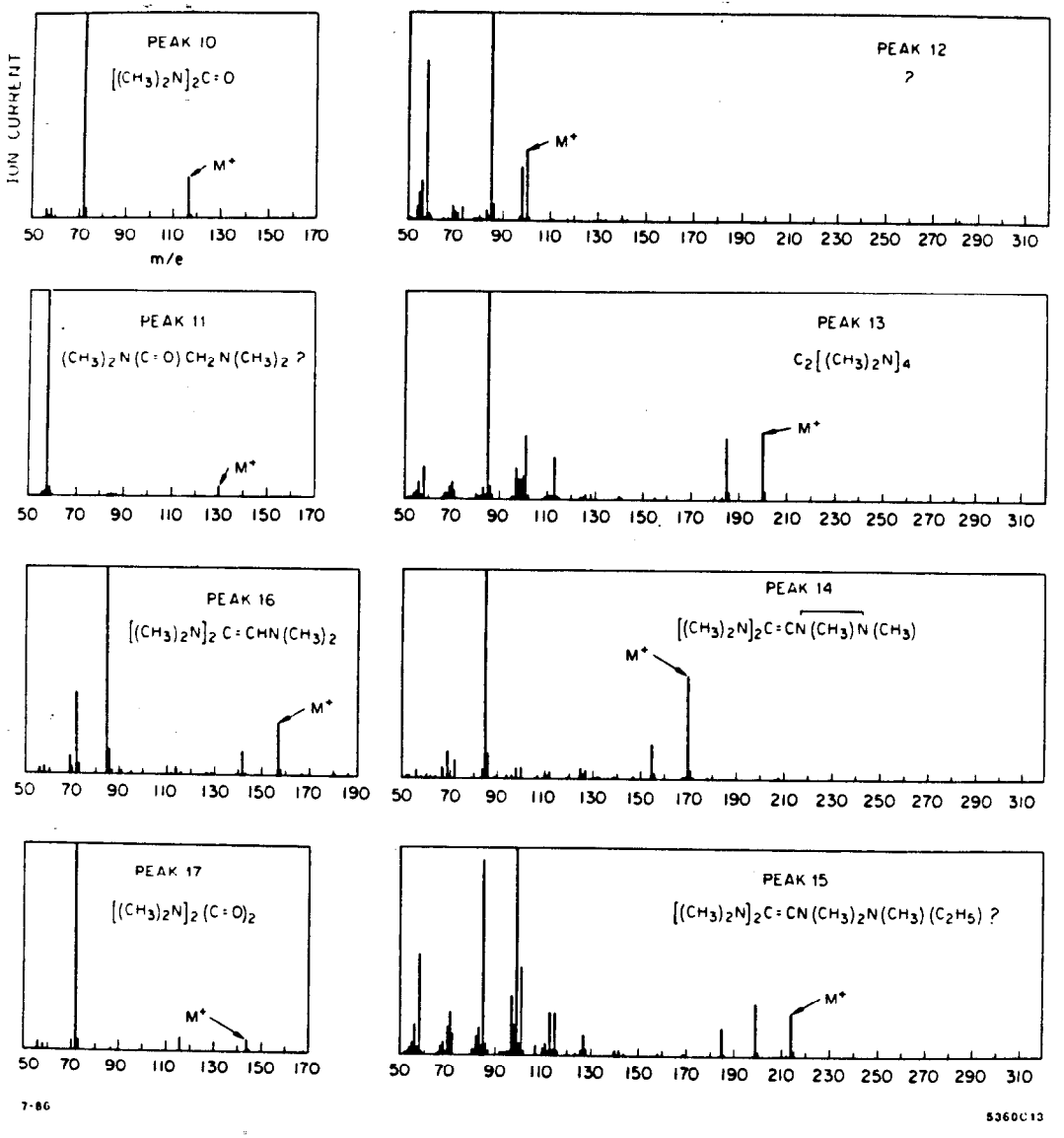
ION CURRENT
PEAK 10
$[(CH_3)_2N]_2C=O$
M+
50 70 90 110 130 150 170
m/e
PEAK 12
?
M+
50 70 90 110 130 150 170 190 210 230 250 270 290 310
PEAK 11
$(CH_3)_2N(C=O)CH_2N(CH_3)_2$?
M+
50 70 90 110 130 150 170
PEAK 13
$C_2[(CH_3)_2N]_4$
M+
50 70 90 110 130 150 170 190 210 230 250 270 290 310
PEAK 16
$[(CH_3)_2N]_2C=CHN(CH_3)_2$
M+
50 70 90 110 130 150 170 190
PEAK 14
$[(CH_3)_2N]_2C=CN(CH_3)N(CH_3)$
M+
50 70 90 110 130 150 170 190 210 230 250 270 290 310
PEAK 17
$[(CH_3)_2N]_2(C=O)_2$
M+
50 70 90 110 130 150 170
PEAK 15
$[(CH_3)_2N]_2C=CN(CH_3)_2N(CH_3)(C_2H_5)$?
M+
50 70 90 110 130 150 170 190 210 230 250 270 290 310
7-86
5360C13

Fig. 5a

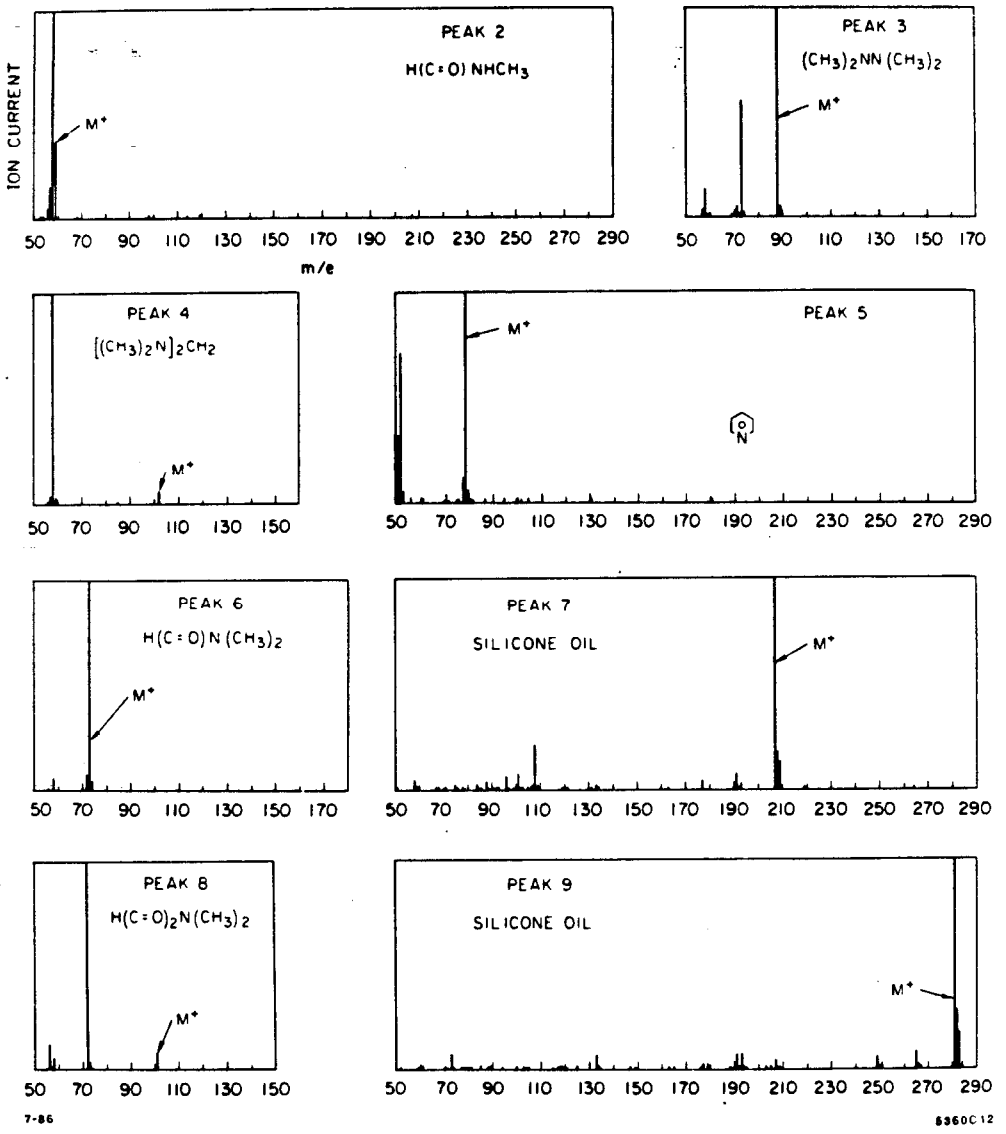
ION CURRENT
PEAK 2
H(C=O) NHCH3
M+
50 70 90 110 130 150 170 190 210 230 250 270 290
m/e
PEAK 3
(CH3)2NN(CH3)2
M+
50 70 90 110 130 150 170
PEAK 4
[(CH3)2N]2CH2
M+
50 70 90 110 130 150
PEAK 5
M+
50 70 90 110 130 150 170 190 210 230 250 270 290
PEAK 6
H(C=O)N(CH3)2
M+
50 70 90 110 130 150 170
PEAK 7
SILICONE OIL
M+
50 70 90 110 130 150 170 190 210 230 250 270 290
PEAK 8
H(C=O)2N(CH3)2
M+
50 70 90 110 130 150
PEAK 9
SILICONE OIL
M+
50 70 90 110 130 150 170 190 210 230 250 270 290
7-86
5360C12

Fig. 5b

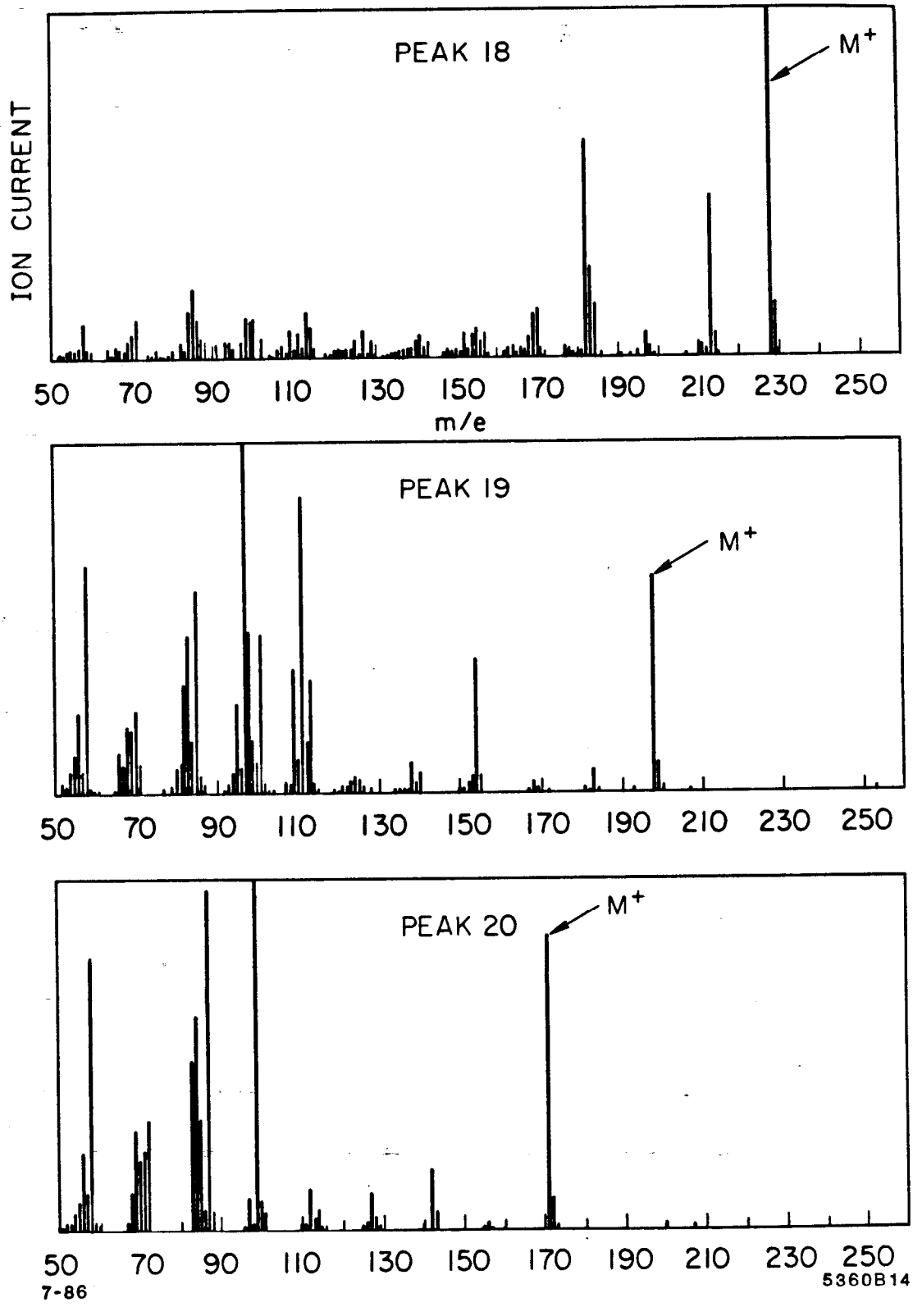
PEAK 18
M+
ION CURRENT
50 70 90 110 130 150 170 190 210 230 250
m/e
PEAK 19
M+
50 70 90 110 130 150 170 190 210 230 250
PEAK 20
M+
50 70 90 110 130 150 170 190 210 230 250
7-86
5360B14

Fig. 5c

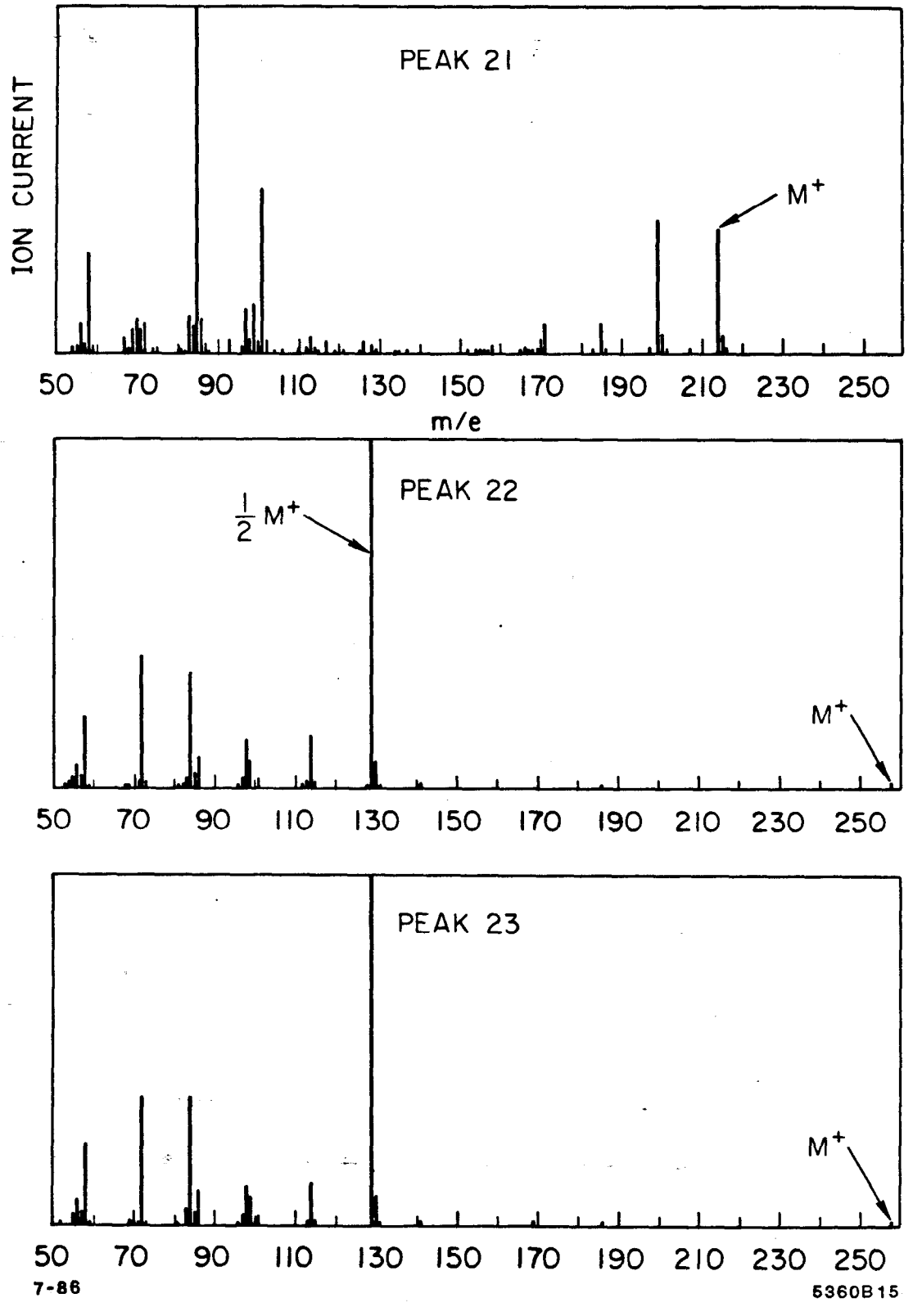
PEAK 21
ION CURRENT
M+
50 70 90 110 130 150 170 190 210 230 250
m/e
PEAK 22
½ M+
M+
50 70 90 110 130 150 170 190 210 230 250
PEAK 23
M+
50 70 90 110 130 150 170 190 210 230 250
7-86
5360B15

Fig. 5d

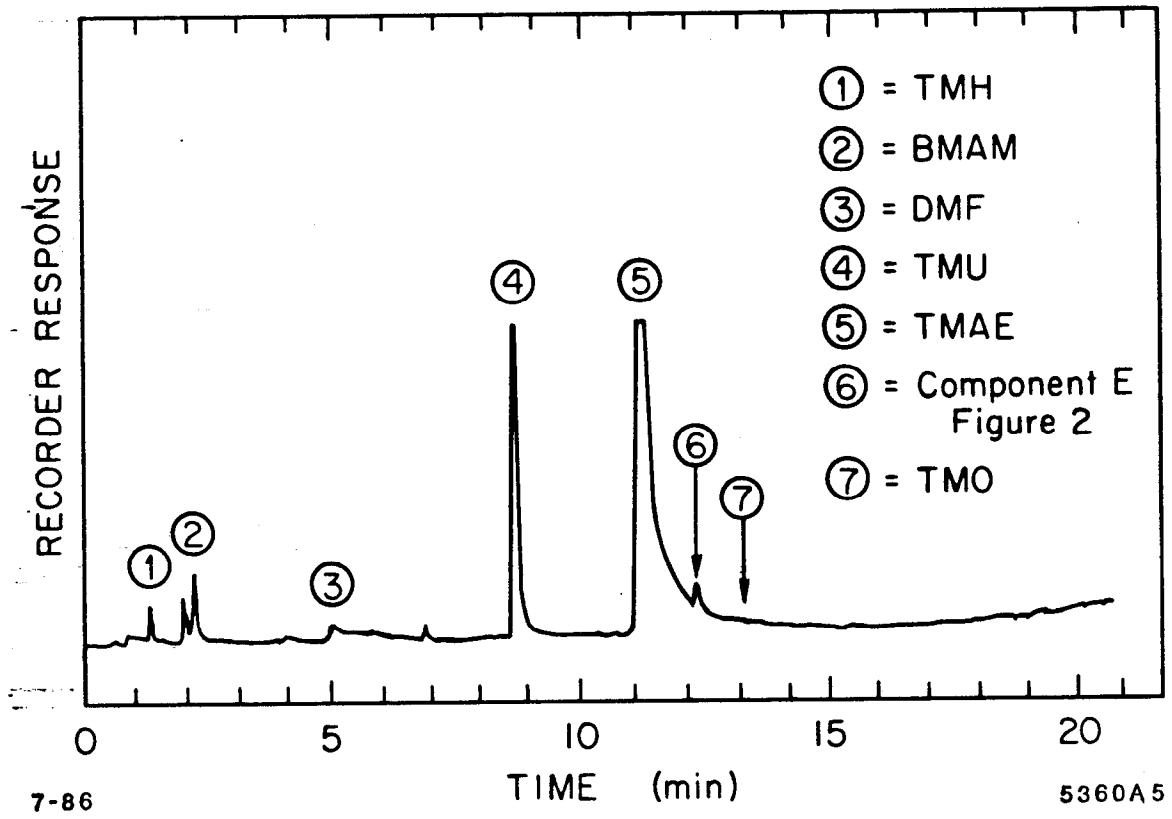
RECORDER RESPONSE
① = TMH
② = BMAM
③ = DMF
④ = TMU
⑤ = TMAE
⑥ = Component E
Figure 2
⑦ = TMO
0
5
10
15
20
TIME (min)
7-86
5360A5

Fig. 6